Electronic supplementary information

Mn^{2+}-doped Cs_2ZnBr_4 scintillator for X-ray imaging

Binbin Su,[a] Kai Han,[2] Zhiguo Xia *[ab]

a.The State Key Laboratory of Luminescent Materials and Devices, Guangdong Provincial Key Laboratory of Fiber Laser Materials and Applied Techniques, Guangdong Engineering Technology Research and Development Center of Special Optical Fiber Materials and Devices, School of Materials Science and Engineering, South China University of Technology, Guangzhou 510641, China.

b. School of Physics and Optoelectronics, South China University of Technology, Guangzhou 510641, China

Table S1. Main parameters of Rietveld refinement of Cs_2ZnBr_4:$x$$Mn^{2+}$.

x(Mn)	Space Group	Cell parameters (Å),	R_p, R_{wp}, R_{exp}, x2
0	*Pnma*	a = 10.19830 (7), b = 7.73996 (8), c = 13.53616 (7), V = 1068.47 (3)	16.5, 11.7, 10.07, 1.34
25%	*Pnma*	a = 10.20406 (0), b = 7.74563 (6), c = 13.54518 (5), V = 1070.57 (5)	17.0, 13.6, 9.17, 2.19

Table S2. Fractional atomic coordinates and isotropic displacement parameters (Å^2) of Cs_2ZnBr_4:$x$$Mn^{2+}$

Atom	*x*	*y*	*z*	*occ*
		0 %		
Cs1	0.6358 (9)	0.25	0.3962 (6)	0.5
Cs2	0.4756 (9)	0.25	0.8298 (4)	0.5
Zn	0.2283 (1)	0.25	0.4166 (1)	0.5
Br1	0.0033 (8)	0.25	0.3995 (4)	0.5
Br2	0.3117 (2)	0.25	0.5902 (5)	0.5
Br3	0.3265 (4)	0	0.3458 (4)	1.0
		25 %		
Cs1	0.6362 (3)	0.25	0.3940 (9)	0.5
Cs2	0.4769 (1)	0.25	0.8317 (8)	0.5
Zn	0.2322 (7)	0.25	0.4144 (0)	0.37503
Mn	0.2322 (7)	0.25	0.4144 (0)	0.12497
Br1	0.0014 (3)	0.25	0.3977 (3)	0.5
Br2	0.3196 (1)	0.25	0.5918 (5)	0.5
Br3	0.3254 (1)	0	0.3458 (1)	1.0

Table S3. The result of ICP-OES measurements for Cs_2ZnBr_4:$x$$Mn^{2+}$

Mn/Zn molar feed ratio	actual Zn concentration (mg/kg)	actual Mn concentration (mg/kg)	actual Mn-to-Zn molar ratio
0.05:0.95 (5%)	99023.1	636.7	0.64%
0.10:0.90 (10%)	98433.4	1268.5	1.29%
0.15:0.85 (15%)	97639.9	1480.1	1.52%
0.20:0.80 (20%)	95294.9	4258.3	4.47%
0.25:0.75 (25%)	88197.3	9490.8	10.76%
0.30:0.70 (30%)	91028.9	8324.5	9.14%

Table S4. PLQYs of Mn^{2+}-doped Cs_2ZnBr_4 with different Mn^{2+} concentrations.

x Mn^{2+}	PLQY
5%	12.66%
10%	19.57%
15%	21.75%
20%	26.73%
25%	58.82%
30%	45.05%

Table S5. PL lifetimes of the green emissions for Mn^{2+}-doped Cs_2ZnBr_4 polycrystalline powders with different Mn^{2+} concentrations.

λ_{ex} = 365 nm, λ_{em} = 526 nm			
x **Mn^{2+}**	**τ_1 (μs)**	**τ_2 (μs)**	**$\tau_{average}$**
5%	25.41	151.58	93.62
10%	20.64	165.18	126.32
15%	15.06	165.25	131.41
20%	14.59	187.71	135.19
25%	14.17	287.80	255.90
30%	9.27	262.86	234.13

Table S6. PL lifetimes of the red emissions for Mn^{2+}-doped Cs_2ZnBr_4 polycrystalline powders with different Mn^{2+} concentrations.

x **Mn^{2+}**	**τ(μs)**
5%	158.30
10%	156.92
15%	156.15
20%	157.55
25%	163.63
30%	157.98

Table S7. Radioluminescence properties of recently reported metal halide scintillators.

Scintillators	Ligh yields (photons/MeV)	Detection limit (nGy_{air}/s)	Spatial resolution (lp/mm)	Imaging	Res
$Cs_3Cu_2I_5$	79279	/	0.32 mm	Films	1
$Cs_3Cu_2I_5$	30000	158		Single crystal	2
Rb_2CuCl_3	16600	88.5	/	/	3
Rb_2CuBr_3	91056	121.5	/	/	4
K_2CuBr_3	23806	132.8	/	/	5
$Cs_2AgI_3:Cu^+$	82900	77.8	16.2	PDMS composite film	6
Rb_2AgBr_3	25600	19	10.2	Film	7
$(C_{38}H_{34}P_2)MnBr_4$	66256	461.1	0.322 mm	PDMS composite film	8
TPP_2MnBr_4	78000 ± 2000	8.8	15.7	Ceramic wafer	9
$(ETP)_2MnBr_4$	35000 ± 2000	103	13.4 l	Transparent glass	10
$(C_{24}H_{20}P_{)2}MnBr_4$	/	608	14.5	TPU composite film	11
$C_4H_{12}NMnCl_3$	50500	36.9	/	SO composite film	12
$(C_8H_{20}N)_2MnBr_4$	24400	24.2	5	SO composite film	12
$(Bmpip)_2Cu_2Br_4$	16000	710	/	/	13
$(DIET)_3Cu_3Br_3$	20000 ± 700	189	11.71	PDMS composite film	14
$(TBA)CuCl_2$	23373	/	/	PVDF composite film	15
$(TBA)CuBr_2$	24134	/	/	PVDF composite film	15
$Cs_2ZnBr_4:Mn^{2+}$	15600	1160	5.06	PDMS composite film	This work

Note: "PMMA", polymethyl methacrylate; "PDMS", polydimethylsiloxane; "TPU", thermoplastic polyurethane; "SO", sucrose octaacetate; "PVDF", polyvinylidene fluoride.

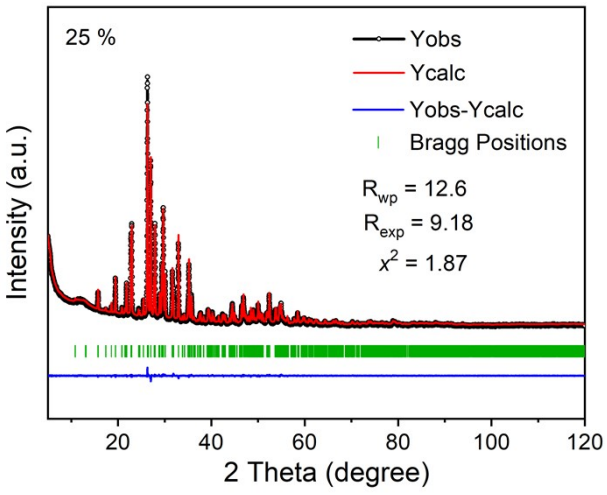

Figure S1. Rietveld refinement of 25%Mn^{2+}-doped Cs_2ZnBr_4 sample.

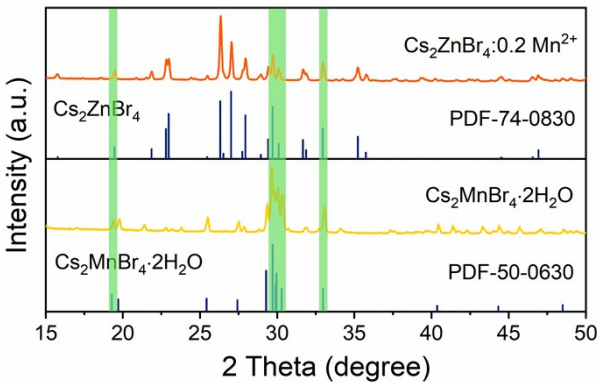

Figure S2. XRD patterns of Cs_2ZnBr_4:25%Mn^{2+} and $Cs_2MnBr_4{\cdot}2H_2O$ samples.

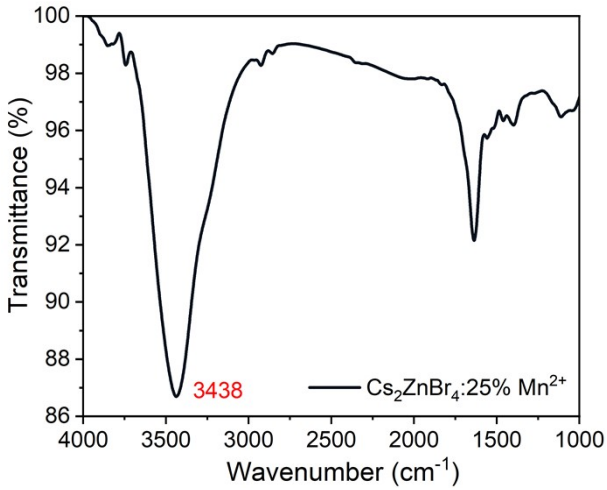

Figure S3. Fourier transform infrared spectrum (FTIR) of Cs_2ZnBr_4:25%Mn^{2+} sample.

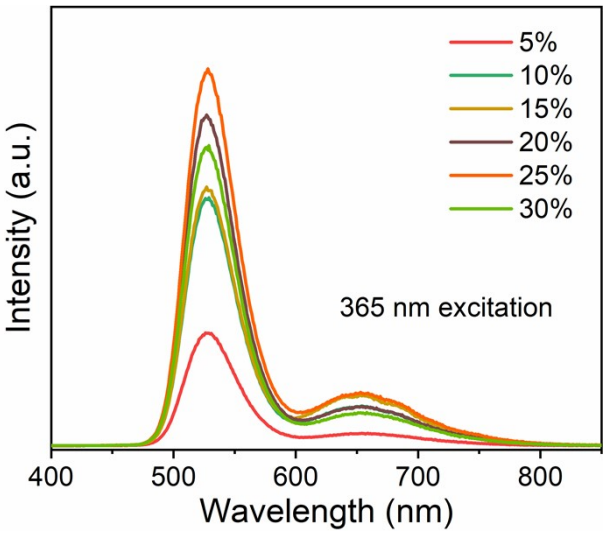

Figure S4. PL spectra of Mn^{2+}-doped Cs_2ZnBr_4 samples with different Mn^{2+} concentrations at room temperature (λ_{ex} = 365 nm).

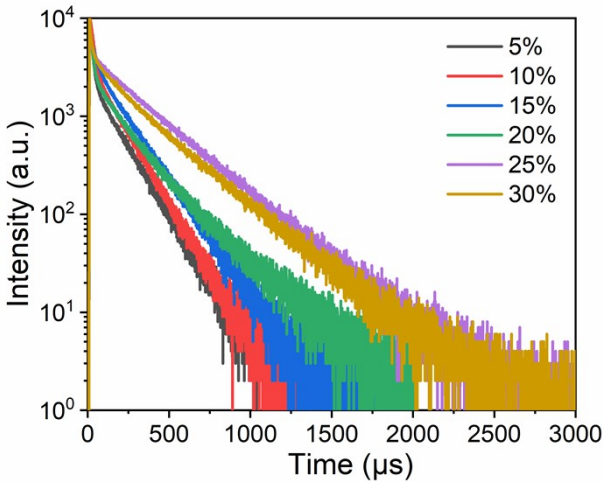

Figure S5. PL decay curves of Mn^{2+}-doped Cs_2ZnBr_4 samples with different Mn^{2+} concentrations at room temperature (λ_{ex} = 365 nm, λ_{em} = 526 nm).

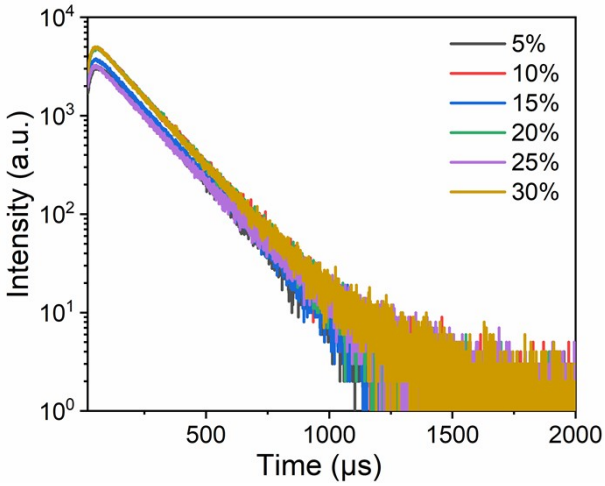

Figure S6. PL decay curves of Mn^{2+}-doped Cs_2ZnBr_4 samples with different Mn^{2+} concentrations at room temperature (λ_{ex} = 365 nm, λ_{em} = 655 nm).

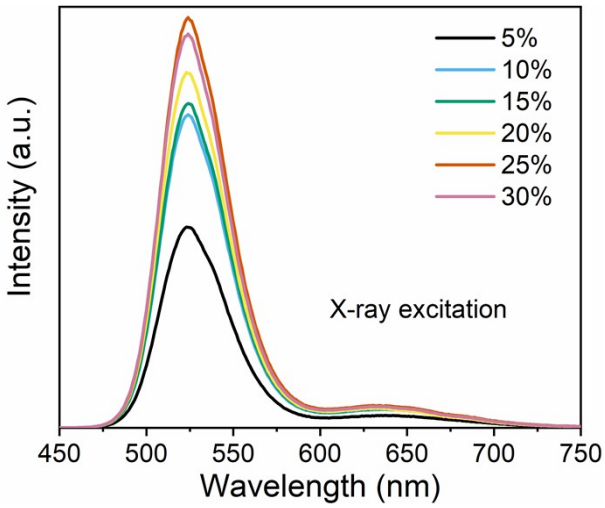

Figure S7. RL spectra of Mn^{2+}-doped Cs_2ZnBr_4 samples with different Mn^{2+} concentrations under X-ray excitation at room temperature (tube voltage: 50 kV; dose rate: 96.09 $\mu Gy_{air}\ s^{-1}$).

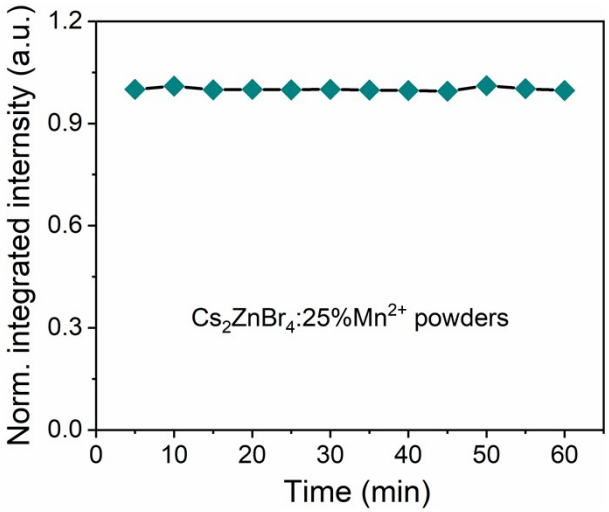

Figure S8. PL stabilities of Cs_2ZnBr_4:25%Mn^{2+} under continuous UV illumination (λ_{ex} = 365 nm).

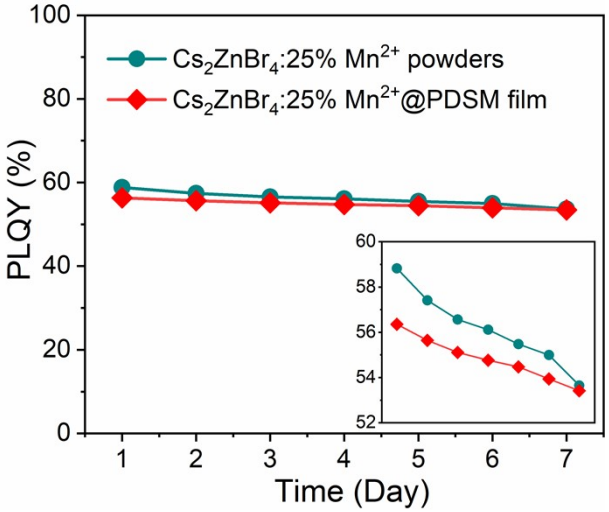

Figure S9. The stabilities of PLQYs of Cs_2ZnBr_4:25%Mn^{2+} polycrystalline powders and Cs_2ZnBr_4:25%Mn^{2+}@PDSM thin film, inset shows the enlarged pattern.

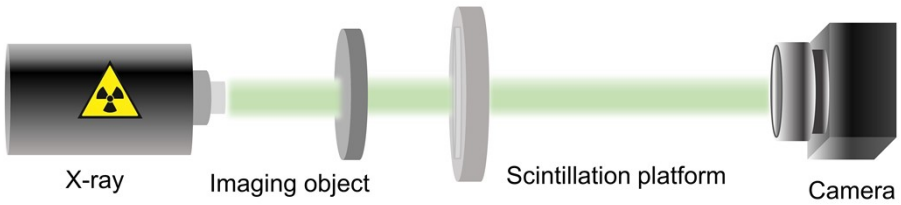

Figure S10. The home-made X-ray imaging system.

Reference

1 L. Y. Lian, M. Y. Zheng, W. Z. Zhang, L. X. Yin, X. Y. Du, P. Zhang, X. W. Zhang, J. B. Gao, D. L. Zhang, L. Gao, G. D. Niu, H. S. Song, R. Chen, X. Z. Lan, J. Tang and J. B. Zhang, *Adv. Sci.*, 2020, **7**, 2000195.

2 Q. Wang, Q. Zhou, M. Nikl, J. W. Xiao, R. Kucerkova, A. Beitlerova, V. Babin, P. Prusa, V. Linhart, J. K. Wang, X. M. Wen, G. D. Niu, J. Tang, G. H. Ren and Y. T. Wu, *Adv. Opt. Mater.*, 2022, **10**, 2200304.

3 X. Zhao, G. D. Niu, J. S. Zhu, B. Yang, J. H. Yuan, S. R. Li, W. R. Gao, Q. S. Hu, L. X. Yin, K. H. Xue, E. Lifshitz, X. S. Miao and J. Tang, *J. Phys. Chem. Lett.*, 2020, **11**, 1873-1880.

4 B. Yang, L. Yin, G. Niu, J. H. Yuan, K. H. Xue, Z. Tan, X. S. Miao, M. Niu, X. Du, H. Song, E. Lifshitz and J. Tang, *Adv. Mater.*, 2019, **31**, e1904711.

5 W. R. Gao, G. D. Niu, L. X. Yin, B. Yang, J. H. Yuan, D. D. Zhang, K. H. Xue, X. S. Miao, Q. S. Hu, X. Y. Du and J. Tang, *ACS Appl. Electron. Mater.*, 2020, **2**, 2242-2249.
6 T. Y. He, Y. Zhou, X. J. Wang, J. Yin, A. Gutiérrez, L., J. X. Wang, Y. H. Zhang, O. M. Bakr and O. F. Mohammed, *ACS Energy Lett.*, 2022, **7**, 2753-2760.
7 M. Y. Zhang, X. M. WANG, B. Yang, J. S. Zhu, G. D. Niu, H. D. Wu, L. X. Yin, X. Y. Du, M. Niu, Y. S. Ge, Q. G. Xie, Y. F. Yan and J. Tang, *Adv. Funct. Mater.*, 2020, **31**, 2007921.
8 L. J. Xu, X. S. Lin, Q. Q. He, M. Worku and B. W. Ma, *Nat. Commun.*, 2020, **11**, 4329.
9 K. Han, K. Sakhatskyi, J. C. Jin, Q. Zhang, M. V. Kovalenko and Z. G. Xia, *Adv. Mater.*, 2022, **34**, e2110420.
10 B. H. Li, Y. Xu, X. L. Zhang, K. Han, J. C. Jin and Z. G. Xia, *Adv. Opt. Mater.*, 2022, **10**, 2102793.
11 K. Y. Xia, P. Ran, W. W. Wang, J. W. Yu, G. P. Xu, K. Wang, X. D. Pi, Q. Q. He, Y. Yang and J. Pan, *Adv. Opt. Mater.*, 2022, **10**, 2201028.
12 T. M. Jiang, W. B. Ma, H. Zhang, Y. Tian, G. Lin, W. G. Xiao, X. Yu, J. B. Qiu, X. H. Xu, Y. Yang and D. X. Ju, *Adv. Funct. Mater.*, 2021, **31**, 2009973.
13 T. T. Xu, Y. Y. Li, M. Nikl, R. Kucerkova, Z. Y. Zhou, J. Chen, Y. Y. Sun, G. D. Niu, J. Tang, Q. Wang, G. H. Ren and Y. T. Wu, *ACS Appl. Mater. Interfaces*, 2022, **14**, 14157-14164.
14 K. Han, J. C. Jin, B. B. Su, J. W. Qiao and Z. G. Xia, *Adv. Opt. Mater.*, 2022, **10**, 2200865.
15 L. Y. Lian, X. Wang, P. Zhang, J. S. Zhu, X. W. Zhang, J. B. Gao, S. Wang, G. J. Liang, D. L. Zhang, L. Gao, H. S. Song, R. Chen, X. Z. Lan, W. X. Liang, G. D. Niu, J. Tang and J. B. Zhang, *J. Phys. Chem. Lett.*, 2021, **12**, 6919-6926.